Energy Conversion and Management: X 18 (2023) 100360

Contents lists available at ScienceDirect

Energy Conversion and Management: X

journal homepage: www.sciencedirect.com/journal/energy-conversion-and-management-x

Techno-economic comparative study of grid-connected PV/reformer/FC hybrid systems with distinct solar tracking systems

Mohamed Dekkiche [a,b], Toufik Tahri [a,b,*], Mouloud Denai [c]

[a] Faculty of Technology, Hassiba Benbouali University, Po Box 151, Chlef, Algeria
[b] Laboratory of Electrical Engineering and Renewable Energy LGEER, Chlef, Algeria
[c] University of Hertfordshire, Hatfield, Hertfordshire, United Kingdom

ARTICLE INFO

Keywords:
Grid-connected system
Photovoltaic panels
Reformer fuel cell
Solar tracker
HOMER

ABSTRACT

The purpose of this study is to analyze and compare the techno-economic performance of grid-connected Hybrid Energy Systems (HES) consisting of Photovoltaic (PV) and Reformer Fuel-Cell (RF-FC) using different types of solar PV tracking techniques to supply electricity to a small location in the City of Chlef, Algeria. The PV tracking systems considered in this study include fixed facing south at four different angles (32°, 34°, 36°, 38°), horizontal-axis with continuous adjustment, vertical-axis with continuous adjustment and a two-axis tracking system. The software tool HOMER Pro (Hybrid Optimization of Multiple Energy Resources) is used to simulate and analyze the technical feasibility and life-cycle cost of these different configurations. The meteorological data, consisting of global solar radiation and air temperature, used in this study was collected from the geographical area of the City of Chlef during the year 2020. This study has shown that the optimal design of a grid-connected hybrid PV/RF-FC energy system with Vertical Single Axis Tracker (VSAT) leads to the best economic performance with low values of Net Present Cost (NPC), Cost of Energy (COE) with a Positive Return on Investment (ROI) and the shortest Simple Payback (SP) period. In addition, from the simulation results obtained, it can be concluded that the Horizontal and Vertical Single-Axis Trackers (HSAT and VSAT) as well as the Dual-Axis Tracker (DAT) are not always cost effective compared to the Fixed Tilt System (FTS). Therefore, it is necessary to carefully analyze the use of each tracker to assess whether the energy gain achieved outweighs the overall shortcomings of the tracker.

1. Introduction

Algeria's electric energy needs are 99 % satisfied from natural gas and oil. The growing energy consumption can make the supply–demand balance problematic for the country's national grid. Also, electricity, produced exclusively from hydrocarbons, is expected to reach between 130 and 150 TWh in 2030 [1]. Thus, to preserve the fossil fuel resources and contribute to sustainable development, it is crucial to diversify the production of electricity with large-scale integration of clean energy in the energy mix. Several studies have been carried out to investigate the potential economic benefit gained from the adoption of grid-connected and stand-alone hybrid energy systems integrating PV systems with sun tracking technologies, Reformer Fuel-Cell, Electrolyser Fuel-Cell, wind turbines, battery energy storage and diesel generator. Several systems configurations have been developed worldwide according to the available renewable energy resources and load requirements. In [2], the authors used an improved Ant Colony Optimization (ACO) algorithm for the optimal sizing of the components of a PV/wind/battery/hydrogen autonomous hybrid system based on real data. The results showed that the proposed hybrid system is cost-effective, and that energy storage plays a vital role in off-grid photovoltaic systems. In [3], a novel energy dispatching strategy based on Model Predictive Control (MPC) was presented for off-grid PV/wind/FC/battery hybrid systems. The simulation results showed that the energy dispatching strategy leads to a higher efficiency, keeping the battery State-of-Charge (SOC) and hydrogen level within the desired operating limits while assuring off-grid load support. In another work [4], an optimal energy management for off-grid hybrid systems under uncertainty was proposed. For this purpose, an autonomous microgrid system consisting of PV/Electrolyser/FC/Batteries was used to analyze the impacts of solar power variability and parametric uncertainty on the system's performance. The results indicate the viability of the strategy for highly variable environmental conditions. A mathematical model of a hybrid power system

* Corresponding author at: Faculty of Technology, Hassiba Benbouali University, Po Box 151, Chlef, Algeria.
E-mail address: t.tahri@univ-chlef.dz (T. Tahri).

https://doi.org/10.1016/j.ecmx.2023.100360
Received 22 December 2022; Received in revised form 2 February 2023; Accepted 3 February 2023
Available online 8 February 2023

Nomenclature

Symbols and Abbreviations

α	Temperature coefficient of power, %/°C
γ	Rated capacity, kW
η	Efficiency, %
C	Cost, USD
CRF	Capacity Recovery Factor
E	Electrical production, kWh/year
F	Fuel consumption rate, m^3/hr
F_0	Curve intercept coefficient, m^3/hr/kW
F_1	Curve slope, m^3/hr/kW
F	Derating factor, %
G	Incident radiation, kW/m^2
LHV	Lower Heating Value, MJ/kg
P	Power, kW
R	Load, kWh/year
T	Temperature, °C
Y	Rated capacity, kW
AC	Alternating Current
COE	Cost of Energy
ACO	Ant colony optimization
ACS	Annual cost of system
DAT	Dual Axis Tracker
DC	Direct Current
DG	Diesel Generators
FC	Fuel Cell
FTS	Fixed-Tilt System
G	Grid
GDP	Gross Domestic Product
GHG	Greenhouse Gases
GN	Gas naturel
HES	Hybrid Energy System
HOMER	Hybrid Optimization of Multiple Energy Resources
HRES	Hybrid Renewable Energy System
HS	Hybrid System
HT	Hydrogen tank
HSAT	Horizontal Single-Axis Tracking
IC	Initial cost
IEA	International Energy Agency
IRR	Internal rate of return
LCOE	Levelized cost of energy
LCOP	Levelized cost of Power
LDR	Light dependent resistor
LNG	Liquefied natural gas
LPSP	Loss of power supply probability
MCFC	Molten carbonate fell cell
MPC	Model Predictive Control
NPC	Net present cost
NREL	National Renewable Energy Laboratory
PEMFC	Proton-Exchange Membrane Fuel Cell
PMS	Power Management Strategy
PV	Photovoltaic
RE	Renewable Energy
RF	Reformer
ROI	Return on investment
SOC	State of charge
SOFC	Solid Oxide Fuel Cell
SOEC	Solid Oxide Electrolyzer Cell
SP	Simple Payback
VSAT	Vertical Single Axis Tracking

Subscript

a	Ambient
ann,tot	Total annualized
c	Cell
cap	System capital cost
cap, ref	Reference system capital cost
i, ref	Reference system annual cash
in	Incoming
on	Outgoing
p	Power
prim	Primary
spec	Specific
STC	Standard Test Condition
T	Current time step
tot,grid,sales	Total grid sales

Superscript

N	Project lifetime, year
O&M	Operating and Maintenance

including a PV system, water electrolyzer, hydrogen tank and Proton Exchange Membrane Fuel Cell (PEMFC) generator was proposed in [5]. The simulation results have shown that the PV/FC/Electrolyser hybrid system was able to track the daily power consumption of the household. In [6], a HRES consisting of PV modules, wind turbines, batteries, fuel cell and a system for hydrogen production, storage was proposed to power a region in Russia with maximum loads of 10 and 100 kW without emissions of greenhouse gas. The simulation results showed that the wind/solar energy system with battery is most efficient for short-term periods whereas if wind and solar resources are absent, hydrogen storage becomes more cost-effective for the studied area. The authors in [7] used HOMER to optimize a stand-alone PV/FC hybrid power system without battery storage to supply a city. The results showed that FCs are a viable and non-polluting alternative to Diesel Generators (DG) with a reduced total maintenance cost. In [8], a hybrid PV/wind/FC power generation system suitable for remote areas was proposed. An electrolyzer and a reformer were also considered in the simulation. The simulation results have shown that the proposed standalone hybrid configuration would be a feasible solution to supply electricity to remote areas. The authors in [9] analyzed the feasibility of two FC/PV/batteries and PV/batteries systems for the electrification of a village and made the comparison with a conventional diesel system. The optimization results and sensitivity analysis have shown that the PV/batteries system is more economical and environmental-friendly solution. In [10], the authors designed an optimal grid-connected PV energy system using HOMER software tool. The optimum result was achieved with a PV inverter size ratio of $R = 1$ and the lowest CO_2 emissions level. Furthermore, the inverter size can be reduced to 68 % of the PV nominal power which reduces the inverter cost. The authors in [11] proposed a wind/PV/FC hybrid system which can deliver power continuously even in the absence of wind and solar energy. FCs are controlled to supply the shortage of electricity when the wind/PV power system cannot satisfy the net demand of electricity. A grid-connected PV/SOFC/Electrolyzer/battery hybrid power system is proposed in [12] to meet the load demands. The results show excellent performance in terms of grid stability, voltage regulation and power quality. Batman et al. [13] performed an evaluation of PV systems to be deployed in the City of Istanbul taking into consideration time-of-use and feed-in tariffs. The results have shown that, by installing PV systems, customers can reduce their electricity bills by more than 40 % per year. Wu et al. [14] developed a hybrid PV/PEMFC/battery stand-alone power system to meet the daily load demand. The hydrogen feeding the PEMFC is produced via a

wastewater treatment process using a heat-integrated fuel processor. The results have shown that the PEMFC power source was reduced from 68 % to 48 %, the battery capacity increased from 10 % to 24 %, and the PEMFC power cost percentage reached 77 %. The authors in [15] proposed a modern energy system for the co-generation of electricity and hydrogen where a combined renewable energy system configuration was incorporated to power a Solid Oxide Electrolyzer Cell (SOEC) installation. The results showed that, the Annual Cost of the System (ACS) was $261,153/year and producing 29.2 tons of H_2/year, with an Levelized Cost of Power (LCOP) of $8.94/kg.$H_2$. An assessment of cost-competitiveness and profitability of fixed and tracking PV systems was done by the authors in [16]. The results of their analysis revealed that fixed and one-axis PV systems are cost-competitive with respect to the electricity price, while two-axis PV systems may not be economically viable, even if the LCOE results are the same, it is better to install one-axis than fixed PV. The authors in [17] have developed a dual-axis solar tracker for a solar panel and evaluated its performance against a fixed system. The tracker used a Light Dependent Resistor (LDRs) to identify the direction of the sun's motion and motors adjust the panel position. The panel with the tracking system showed average monthly gains ranging from 17.20 % to 31.1 %. The performance of three different tracking modes of a PV system is presented in [18]. The results found that in the continuous and three positions tracking modes, the solar gain is about 30 % better than that in the fixed mode in clear weather conditions. In addition, it has been shown that the total electrical power gain of the three positions tracking modes is about 23.4 % better than that of the fixed mode when the power consumption of the tracking system is included. Yaichi et al. [19] found that a discontinuous East-West two-position tracking system (DT-2P) is a good solution for balancing the benefits and drawbacks of continuous tracking and fixed systems. They implemented an experimental water pumping system test bench with DT-2P PV and fixed PV to assess its performance. The results showed that despite its simple design, DT-2P approximates the behavior of a continuous tracker. Xuan et al. [20] studied two grid-connected PV systems with 250 W solar panels to assess the efficiency improvement of a single-axis sun tracking system. The experimental results showed that the total energy consumption of the tracking system was about 2 to 8 % of the energy generated by the grid-connected PV system. Alktranee et al. [21] proposed a single-phase grid-connected PV system using dual-axis solar tracking (DAST) to increase power generation. The results revealed that the fixed PV system can supply over 84.8 % of the total electricity demand while DAST-PV system can satisfy the total load demand. A low-power grid-connected/PV system based on automatic sun tracking is designed by Liu et al. [22]. To increase the precision of the sun tracking, the authors adopted a hybrid tracking method and used pin-cushion two-dimensional position sensitive detector with four photosensitive elements. The experimental results indicated an enhanced performance of the tracking system and an increase in the efficiency of the overall system. The author in [23] presented a techno-economic and sensitivity modelling of a PV/Wind/FC energy system backed up with both hydrogen and battery storage, with seven solar photovoltaic tracking techniques. The authors in [24] designed a grid-connected PV/FC hybrid electrical system and discussed the influence of four main PV monitoring techniques on the technical and economic performance of the system. The authors used « HOMER Pro » in their simulation study and found that the optimal design of a grid-connected PV/FC Hybrid Renewable Energy System (HRES) was based on a single-axis vertical tracker which produced the lowest NPC and LCOE.

In this paper, we present a comparative analysis of different configurations of grid-connected PV/Reformer/FC. The reformer transforms natural gas into hydrogen to supply FCs which produce electrical energy. Several PV tracking systems are studied and compared to determine the most efficient and cost-effective configuration. The scenarios of grid-connected Hybrid Energy Systems (HES) consisting of Photovoltaic (PV) and Reformer Fuel-Cell (RF-FC) using different types of solar PV tracking techniques are:

1st scenario is fixed facing south at four different angles: 32°, 34°, 36°, 38°(FTS);
2nd scenario is horizontal-axis with continuous adjustment (HSAT);
3rd scenario is vertical-axis with continuous adjustment (VSAT);
4th scenario is two-axis tracking system (DAT).

The main contributions and innovations of this work can be summarized as follows: (i) Comprehensive feasibility study of a Reformer/FC system supplied by natural gas to operate as a back-up power supply for the grid-connected hybrid power system to supply electricity to a small agglomeration in the City of Chlef, Algeria (ii) Analysis of different types of solar PV tracking techniques including fixed facing the south at four different angles (32°, 34°, 36°, 38°), horizontal-axis with continuous adjustment, vertical-axis with continuous adjustment and a two-axis tracking system (iii) Comparative techno-economic performance of grid-connected Hybrid Energy Systems (HES) consisting of Photovoltaic (PV) and Reformer Fuel-Cell (RF-FC) based on different types of solar PV tracking techniques using HOMER Pro software (iv) Assessment of the HES based on several technical, environmental and economic factors, such as PV power production, energy excess, renewable energy penetration, annual energy purchased/sold from/to the grid, GHG emissions, project NPC and COE, Internal Rate of Return (IRR), Return on Investment (ROI), lifetime project cost and Simple Payback (SP).

The remaining of the paper is organized as follows: Section 2 presents and describes the hybrid energy system used in this study. Section 3 introduces the HOMER Pro software and defines the input data to be entered into the program. The results obtained from the various tracking systems and the techno-economic analysis carried out to determine the optimum system in terms of maximizing energy production are presented and discussed in Section 4. Finally, the conclusions of the paper are summarized in Section 5.

2. Studied hybrid energy system

A multi-source system combining fossil fuel-based power generation and renewable energy sources connected to grid is considered as a viable solution to optimize electricity production both from a technical and economic point of view. One of the most challenging problems in the design of hybrid energy system is the optimization of the energy components sizes, with respect to the cost of energy and the overall performance of the system. The hybrid electric energy production system considered in this study is presented in Fig. 1. It consists of a PV installation with a sun tracking system and a reformer (RF) that produces hydrogen using natural gas as fuel. The FC supplies electricity to the load during periods when solar energy is not available. This hybrid system is designed to supply electricity to a small neighborhood in the City of Chlef (Algeria). In this study, constant prices are used for the sale and purchase of electricity to/from the grid because these prices are subsidized and do not fluctuate. In HOMER, the purchase rates for grid electricity are $0.038/kWh and the sale rates are $0.144/kWh [25].

The limitations of using the HOMER software in this study can be summarized as follows:

- The user needs to pre-determine the possible configuration of the hybrid energy system.
- The quality of the input data is crucial (weather parameters and load requirement and the desired location).
- A skillful criterion is necessary for convergence towards the right solutions.
- HOMER cannot guess key values or dimensions if they are not available.

2.1. PV system and sun tracking technologies

Solar PV modules can be installed either on fixed supports on the

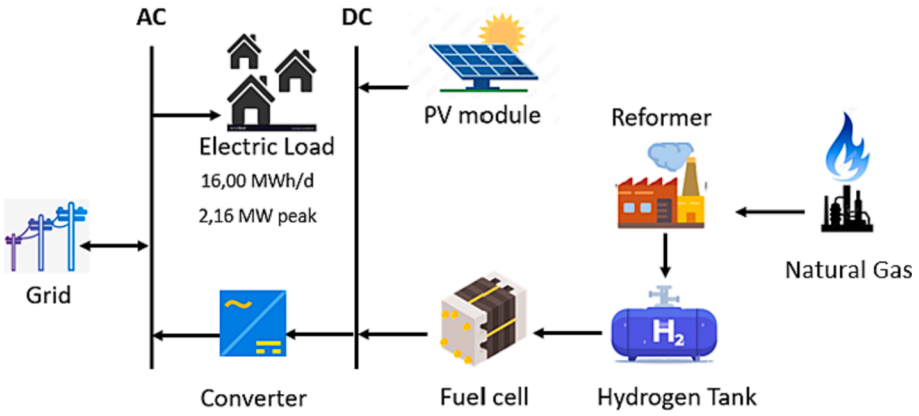

Fig. 1. Grid-connected PV/RF/FC hybrid system considered in this study.

ground or on mobile sun tracking systems called trackers which follow the position of the sun throughout the day to maximize the production of electricity.

In HOMER, Eq. (1) is used to calculate the PV output power (P_{PV}) [26]:

$$P_{PV} = \gamma_{PV} f_{PV} \left(\frac{G_T}{G_{T,STS}}\right)\left[1 + \alpha_p \left(T_C - T_{C,STS}\right)\right] \quad (1)$$

where γ_{PV} is the rated capacity of the PV array, i.e. its power output under standard test conditions [kW], f_{PV} is the PV derating factor [%], G_T denotes the solar radiation at the current time step [kW/m^2], $G_{T,STC}$ represents the incident radiation at standard test conditions [1 kW/m^2], α_p is the temperature coefficient of power [%/°C], T_C is PV cell temperature at the current time step [°C], $T_{C,STC}$ is PV cell temperature under standard test conditions [25 °C].

From Eq. (1), the power generated by a PV system is influenced by several factors, including the temperature of the PV cells and the intensity of the solar radiation. Table 1 presents the manufacturer's technical and economic characteristics of the PV module considered in this study. The PV system is based on the monocrystalline solar module from Condor Electronics Company (CEM100M-36) with peak capacities of 100 W [27,28]. The following parameters of the photovoltaic panels must be entered into HOMER: the type of current (DC), the lifetime (25 years), the losses caused by heat and fouling (80 %) and the reflectivity of the ground (20 %).

Most of the solar PV panels are installed on a fixed mounted system, with a fixed tilt angle. PV tracking techniques are a mechanism to adjust solar panels towards sun's rays to maximize the amount of solar radiation collected by the PV system. The four tracking systems used in this work are presented in Fig. 2 and are briefly described blow.

1. Fixed-Tilt Solar panel (FTS): The PV panel is fixed with four different tilts of 32°, 34°, 36° and 38° and a fixed azimuth of 0° (Fig. 2(a)),
2. Horizontal Single-Axis Tracking (HSAT): The PV turns around the horizontal axis (east–west). The tilt angle is adjusted to match the angle of incidence, while the azimuth is fixed at 0° (Fig. 2(b)),
3. Vertical Single Axis Tacking (VSAT). The PV turns around the vertical axis (north–south). The tilt is fixed; however, the azimuth is simultaneously adjusted to match the angle of incidence (Fig. 2(c)).
4. Dual Axis Tracker (DAT). The PV turns simultaneous on the horizontal and vertical axis. Thus, the angle of incidence is always perpendicular to the surface of the panels (Fig. 2(d)).

The different tracking systems costs, excluding the cost of the PV module, are given in Table 2.

Table 1
PV parameters [27,28].

Capacity (kW)	1
Capital cost (US$)	796
Replacement cost (US$)	796
Operation & Maintenance cost (US$/year)	00
α_p (%/°C)	−0.41
Efficiency (%)	13

2.2. Reformer

Large-scale industrial hydrogen production by methane reforming is the most efficient and widespread process for the production of hydrogen (H_2). It is based on the transformation of fossil energy (e.g. natural gas (CH_4)) through a chemical reaction as described by Eq. (2). This process is used to supply hydrogen to FCs [30]:

$$CH_4 + CO_2 \rightarrow 2\ CO + 2\ H_2 \quad (2)$$

There are several methods of reforming natural gas. One of the mature production processes is Steam Reforming which uses a burner operating at temperatures above 650 °C to produce a mixture of 80 % H_2 and 20 % CO_2 at an efficiency of 80 % [31]. Fig. 3 represents a simplified diagram which describes the reforming process of natural gas to produce H_2.

The energy conversion mechanism can be poisoned with carbon, which decreases the efficiency of the FC and shortens its lifetime. The efficiency of the reformer lies in its performance during the conversion of the fuel into hydrogen. From this value, HOMER calculates the amount of fuel required by the reformer to produce the required quantity of hydrogen. Eq. (3) is used to calculate this efficiency (η_{ref}) [33]:

$$\eta_{ref} = \frac{LHV_{on}}{LHV_{in}} \times 100 \quad (3)$$

where η_{ref} is the reformer efficiency [%], LHV_{on} denotes the outgoing net calorific value [MJ/kg], LHV_{in} is the incoming net calorific value [MJ/kg].

Table 3 presents the technical and economic characteristics of the reformer used in the proposed system with type of current (DC), lifetime (25 years) [34,35] and different capacities from 100 to 1,000 kg/h are considered. These parameters were included in the calculations performed by HOMER, with natural gas as fuel at an average price of \$0.031/m^3 [36].

2.3. Hydrogen storage tank

A hydrogen tank is used to store the hydrogen gas produced by the reformer which will supply the FCs. Hydrogen has the highest energy

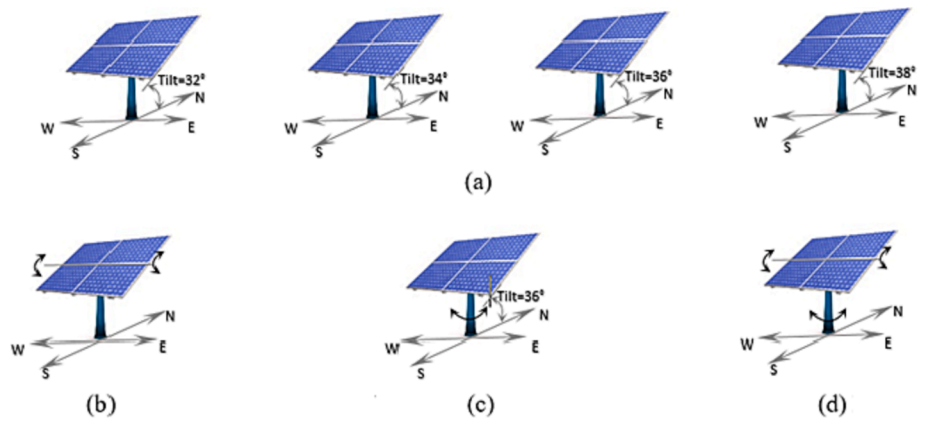

Fig. 2. PV tracking systems (a) Fixed-facing at four different tilt angles (b) Horizontal single-axis solar tracker, (c) Vertical single-axis solar tracker, (d) Dual-axis tracker.

Table 2
Tracking systems cost [29].

No.	Tracking system	Capital cost ($/kW)
1	Fixed-facing tilt angles	0
2	South orientation and single axis horizontal tracking	870
3	Fixed tilt and vertical single axis tracking	255
4	Dual axis tracker	1,000

content per mass amongst all fuels, and can be stored as compressed gas, in chemical form and at very low temperatures (≤20°K) [37]. It is an environmentally friendly fuel since the only derived product, when it is converted in a FC, is water [38]. The initial amount of hydrogen can also be defined in HOMER in kilograms or as a percentage of the tank size. In our work, the initial hydrogen quantity was 10 % of the tank size. Table 4 indicates the capital and replacement costs of the tank, in addition to the installation, yearly maintenance, and the operating costs, are input to HOMER to allow the economic metrics of the system to be calculated.

2.4. Fuel cell

The FC is an electrochemical device that produces electrical energy in the form of direct current (DC) by combining hydrogen with oxygen through a chemical reaction. A single FC can generate high power with an efficiency of 60 % i.e. more than conventional combustion engines which have an efficiency of about 40 % [40]. As a result, FCs can be used to supply larger loads, for example cities. Some FC systems generate significant amounts of heat, especially those that operate at high temperatures, such as solid oxide (SOFC) and molten carbonate (MCFC) systems. Steam and hot water can be produced by converting energy excess to electricity via a gas turbine or using other techniques. The system's overall energy efficiency is increased through heat exchange and recovery [41–43]. The choice of FC type will primarily depend on the size of the power generating plants. Although there is no option to include a special type of FC, the price range and properties considered in this analysis are those of PEMFC. The technical and economic specifications are: capital costs of $3,000/5kW, replacement costs of $2,500/kW, manual and maintenance costs of $0.08 per year while the life cycle is 40,000 h [24].

The fuel curve describes the amount of fuel consumption rate (F) that the FC consumes to produce electricity. In HOMER software, the fuel curve is assumed to be a straight line. Eq. (4) gives the FC fuel consumption in m^3/hr as a function of its output power [44]:

$$F = F_0.Y_{FC} + F_1.P_{FC} \tag{4}$$

where F_0 is the FC curve intercept coefficient [m^3/hr/kW], F_1 is the FC curve slope [m^3/hr/kW], Y_{FC} denotes the rated capacity of the FC [kW] and P_{FC} represents the output power of the FC in this time step [kW].

The specific fuel consumption is calculated by HOMER using Eq. (5) [44]:

$$F_{spec} = \frac{F_{tot}}{E_{FC}} \tag{5}$$

where F_{spec} is the specific fuel consumption [m^3/kWh],F_{tot} is the total annual generator fuel consumption [m^3/yr], and E_{FC} represents the total annual electrical production of the generator [kWh/yr].

Table 3
Reformer parameters [34,35].

Capacity (kW)	1
Capital cost (US$)	3,500
Replacement cost (US$)	3,200
Operation & Maintenance cost (US$/year)	200
LHV (MJ/kg)	45
Density GN (kg/m^3)	0.790
Efficiency (%)	68.60

Table 4
Hydrogen tank parameters [39].

Capacity (kg)	1
Capital cost (US$)	600
Replacement cost (US$)	400
Operation & Maintenance cost (US$/year)	3
Lifetime	25

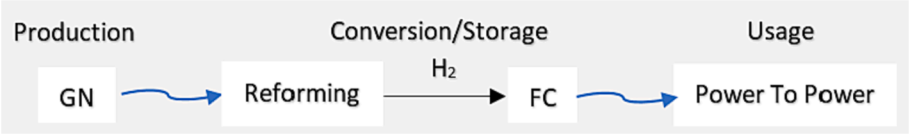

Fig. 3. Simplified reforming process [32].

2.5. Inverter

The PV-FC hybrid power system generates a DC current which is converted to AC to supply the load. The sizing of the DC-AC converter is optimized by HOMER based on the power flow from PV and FC systems. For a 1 kW system, the installation and replacement costs are respectively $400, $200 and $100/year cost for operation and maintenance (O&M). Four different sizes of inverters (0, 2,000, 2,050 and 2,100 kW) are considered in the simulation study. In addition, the life cycle of 20 years was assumed for the power converter with an efficiency of 95 % [7].

3. Modeling of the HES in HOMER

HOMER is considered as a world benchmark in microgrid software, based on decades of listening to the needs of users worldwide. HOMER's optimization and sensitivity analysis algorithms allow the user to assess the economic and technical feasibility of a large number of technological options and to take into account the uncertainty of technological costs, availability of energy resources and other variables [45]. HOMER software is a time-step simulator which uses hourly load and weather data inputs for renewable energy system assessment; HOMER performs the optimization of renewable energy systems based on the Net Present Cost based on some given set of constraints and sensitivity variables. It simulates the operation of a system by making energy balance calculations for each of the 8760 h/yr, for each hour it compares the electric demand in the hour to the energy that the system can supply in that hour, and calculates the flow of energy to and from each component of the system. At the end of the simulation, HOMER presents the results of the different system configurations classified according to their total NPCs. HOMER then repeats this optimization process for each sensitivity variable.

The design and optimisation of the HES using HOMER has three main steps:

(i) *Project Inputs*: Economics (equipment cost information, interest rate, etc.), load profile (average energy consumption of the load), site specific renewable resources (wind speed and solar irradiance data of the area of interest), HES components (PV, wind turbine, diesel generator, battery storage, etc.) and parameters.
(ii) *Analysis*: Simulation, optimisation, sensitivity.
(iii) *Output and Results*: List of feasible configurations with performance details, sizing of individual HES components, financials and economic feasibility.

The methodology applied to determine the optimum HES for the present study location is described by the flowchart of Fig. 4.

3.1. Project input data

The design of the HES depends on some important variables to optimize the cost of the system and the size of the components. Therefore, before designing the model of the system, parameters such as location, solar irradiance, ambient temperature, and load demand must be evaluated.

3.1.1. Study location

The proposed HES to supply electricity to a neighborhood in the City of Chlef (Algeria), is tested using a estimated load demand profile and real weather data. The location of the neighborhood is 36° 08″ North latitude and 1° 20″ East longitude as illustrated in Fig. 5 [46]. The estimated life of the project is approximately 25 years.

3.1.2. Potential of renewable resources

It is essential to assess the climatic parameters of the location considered in this study such as global solar radiation and ambient temperature to be used in HOMER to optimize the grid-connected HES. The meteorological data were collected during one-year period from 1st January to 31st December 2020 using the "Vantage Pro 2" weather station installed at the University Hassiba Benbouali of Chlef.

3.1.3. Solar radiation

The global solar radiation recorded on a horizontal surface in the region of Chlef during 2020 is shown in Fig. 6 Daily average values of

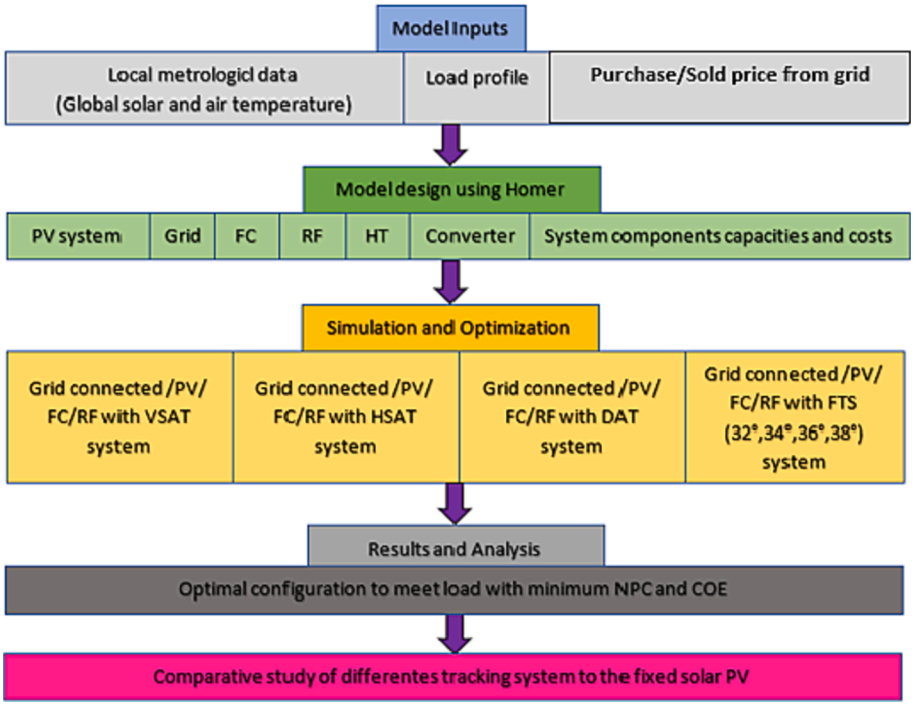

Fig. 4. Flowchart describing the optimization and modeling stages for the design of the HES.

Fig. 5. Geographical location of Chlef (Algeria).

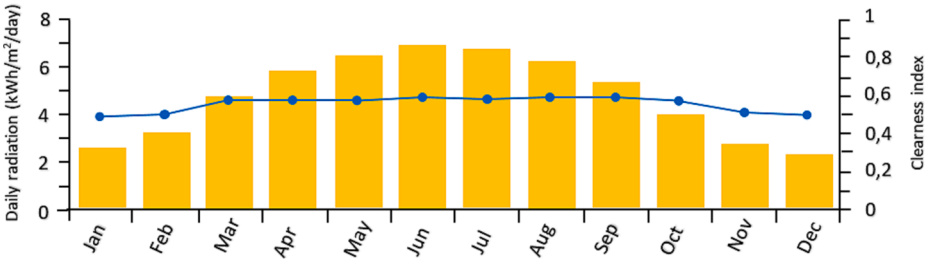

Fig. 6. Monthly mean radiations and clearness index at the City of Chlef in 2020.

global irradiation exceed 4.62 kWh/m^2/day during the period from March to September 2020 while less solar radiation is expected from October to February 2020. In addition, HOMER software can generate the clearness index from the solar radiation data (Fig. 6). The clearness index is the percentage of solar radiation that passes through the atmosphere and reaches the surface of the earth. It is therefore a measure of the transparency of the atmosphere. The clearness index is a dimensionless number between 0 and 1, defined as the surface radiation divided by the extraterrestrial radiation [47–49]. Typical average monthly values of the clearness index are between 0.49 in January (very cloudy) to 0.59 in September (very sunny), which is an indication of the availability of relatively high potential solar power in the studied location.

3.1.4. Ambient temperature

The temperature greatly affects the output power of the PV system and reduces the efficiency. The average monthly air temperature ranges from 10.75 °C to 31.17 °C with an annual average of 20.54 °C as shown in Fig. 7. The ambient temperature is above the average value from May to October and is maximum in July. The remaining months show a low average value, with the lowest average value recorded in January.

3.1.5. Load profile

To have an accurate energy consumption dataset, it is essential to consider the population size and the various economic activities of the studied location. The population is estimated at 10,000 inhabitants and energy consumption is mainly from residential households and commercial activities such as shops, services, etc. Making an optimal estimate is crucial to avoid over sizing the HES which increases the cost or under sizing the system which may lead to power outages [7]. In this study, the load is modeled with average daily demand estimated at 16 MWh/day and demand peaks of nearly 2.163 MW corresponding to the month of August due to AC loads with a load factor of 0.31; that is, the average load divided by the peak load over a 24 h period. The daily load profile for all months is shown in Fig. 8 which shows high electricity consumption in the month of August due to the extensive use of air

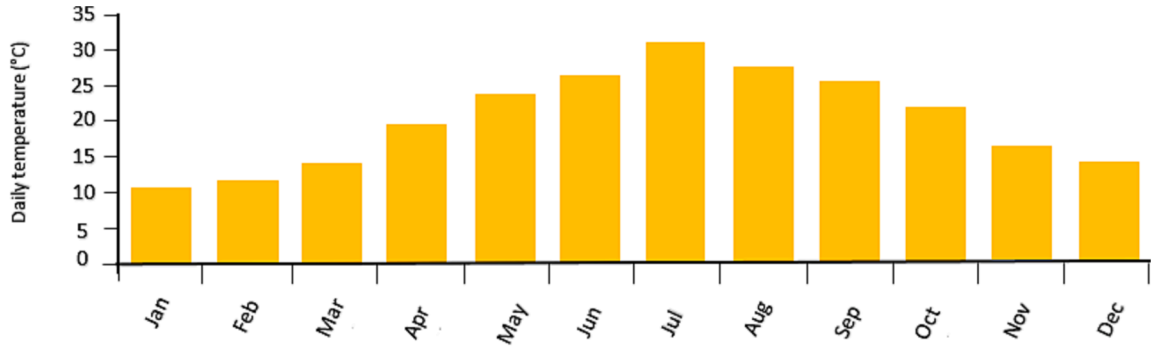

Fig. 7. Monthly average ambient temperature in the City of Chlef.

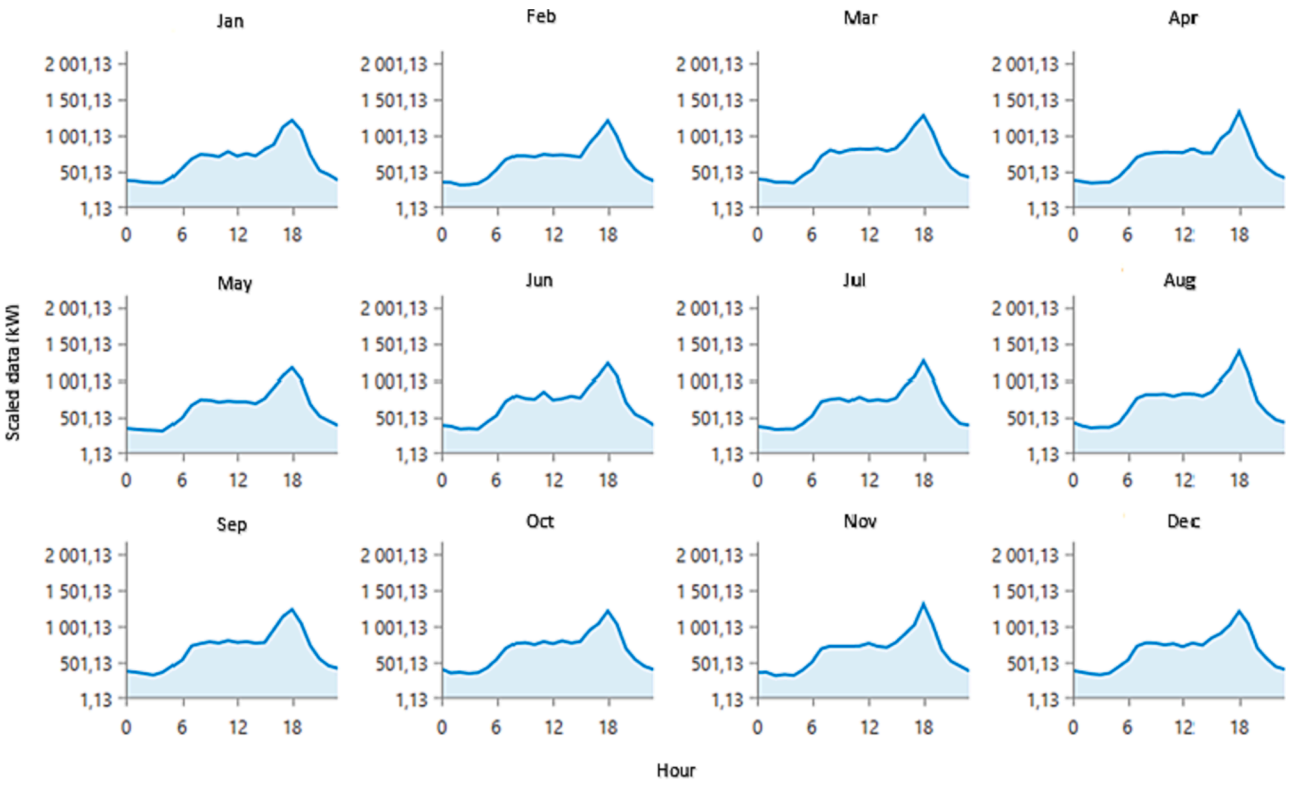

Fig. 8. Daily load profile.

conditioning.

4. Results and discussion

In this section, the results and discussion of different grid-connected PV/Reformer/FC hybrid systems designs are presented. Four cases of fixed system of angles (32°, 34°, 36°, 38°), and three tracking system: horizontal-axis with continuous adjustment, vertical-axis with continuous adjustment and a two-axis tracking are examined to determine the most technically and economically efficient system. The results obtained from the 13,860 simulations carried out by HOMER are examined in our study. Many technical and economic factors, such as PV power generation, energy excess, renewable energy penetration, energy purchased/sold from/to the grid, lifetime project cost and cost of energy and so on, are considered. The Optimization Results Table lists all the feasible configurations. HOMER shows the top-ranked system configurations according to Net Present Cost (NPC).

4.1. Technical comparison of different PV tracking systems

The overall performance of the grid-connected hybrid PV-RF-FC system has been carefully analyzed for different PV tracking techniques. From the point of view of total annual PV power generation, as shown in Fig. 9, VSAT system has the highest generated power, followed by HSAT, DAT and the four cases of fixed angle systems of 36°, 38°, 32°and 34° corresponding to 9.232 GWh/year/year, 9.096 GWh/year/year, 8.951 GWh/year/year, 7.823 GWh/year/year, 7.813 GWh/year/year 7.690 GWh/year/year and 7.628 GWh/year/year, respectively. Also, the VSAT produced respectively 1.49 %, 3.14 %, 18.01 %, 18.16 %, 20.05 % and 21.02 % more power than the HSAT, the DAT and the FTS (36°, 38°, 32°, 34°).

Excess of electrical energy occurred when PV power generation exceeds the load consumption. In our case, the surplus of electricity will be sold to the grid. Fig. 9 shows that the highest excess of energy occurs with the HSAT system with a production of 2.528 GWh/year/year

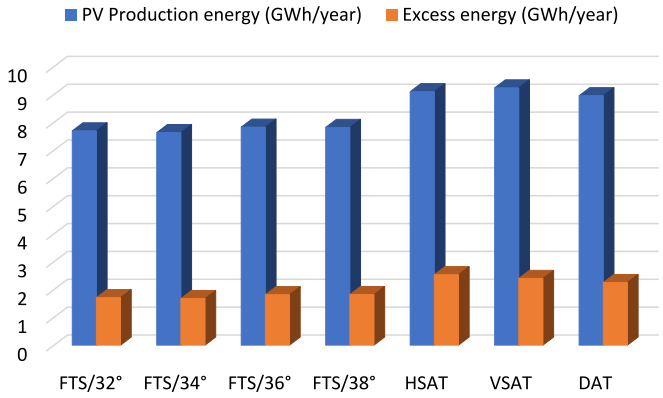

Fig. 9. Energy production and excess of one year for different PV tracking techniques.

followed by the VSAT, DAT and FST of 38°, 36°, 32°and 34° with production of 2.394 GWh/year/year, 2.245 GWh/year/year, 1.814 GWh/year/year,1.811 GWh/year/year, 1.704 GWh/year/year and 1.671 GWh/year/year respectively.

PV penetration ratio is defined as the average power output of the PV array divided by the average primary load. It is an important criterion considered to study the grid-connected PV/RF/FC hybrid systems with tracking techniques. These tracking systems play an important role in increasing PV capacity penetration into the grid as shown in Fig. 10. In this study, the maximum PV penetration is provided by the VSAT system with 158 %, followed by HSAT, DAT and the four cases of fixed angle systems of 36°, 38°, 32°and 34° corresponding to 156 %, 153 %, 134 %, 134 %, 132 % and 131 % respectively.

Furthermore, it is also preferable to analyze the energy sold and purchased to and from the electricity grid over one year, considering all three PV tracking techniques (HSAT, VSAT, DAT) and the four fixed

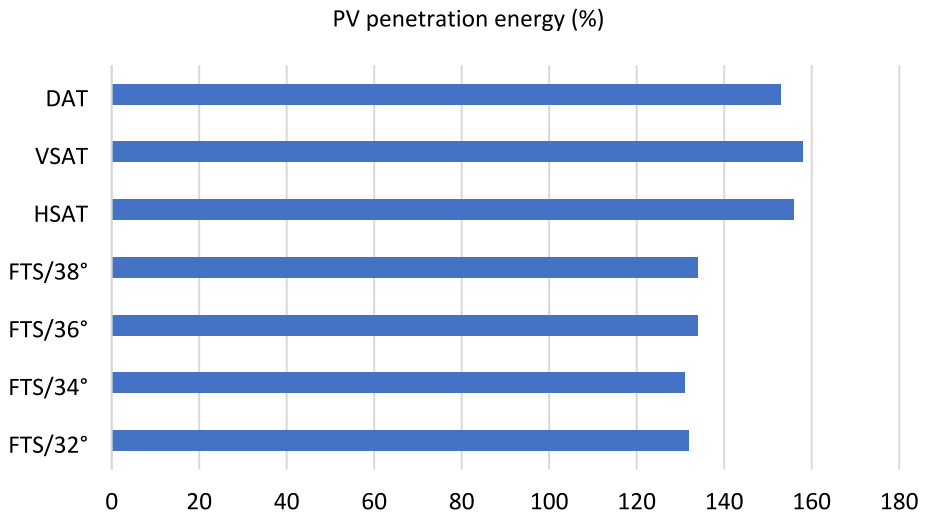

Fig. 10. PV penetration of one year for different PV tracking techniques.

angle system cases (32°, 34°, 36°, 38°). The total annual energy purchased from and sold to the grid compared to the total annual load is illustrated in Fig. 11, which shows that the FTS of 34°, 38°, 32°and 36° receives the highest annual purchase of energy, estimated at 3.069 GWh/year/year, 3.061 GWh/year/year, 3.059 GWh/year/year, 3.057 GWh/year/year respectively, followed by HSAT, DAT and VSAT corresponding to 2.873 GWh/year/year, 2.870 GWh/year/year and 2.810 GWh/year/year, respectively. VSAT gets the highest energy sold back to the grid followed by DAT, HSAT and FST. In terms of total annual energy sold back to the grid, VSAT sold 3.577 GWh/year/year, and DAT, HSAT and FST are ranked next, with 3.502 GWh/year/year, 3.391 GWh/year/year and 3.011 GWh/year/year, respectively.

According to the International Energy Agency (IEA), Algeria is ranked 9th among the ten main exporting countries of liquefied natural gas (LNG) and is ranked the fourth oil producers in Africa [50,51]. Its economy is entirely dependent on oil and gas exports, contributing 50 % of its Gross Domestic Product (GDP). Natural gas is the main source of electricity generation, and this is raising major environmental concerns as Algeria contributes with 2.8 % of global emissions and 70.40 % of these are from CO_2 [52]. Algeria plans to reduce its GHG emissions, by increasing its renewable energy production capacities up to 22,000 kW by 2030, i.e., to achieve 40 % of electricity production from renewable sources (37 % solar, 3 % wind) [53]. PV panels can be designed to follow the sun to maximize incident solar radiation and help increase PV productivity, PV penetration, reduce fossil fuel dependence and CO_2 emissions. Fig. 12 shows that VSAT produces the lowest CO_2 emissions, followed by DAT, HSAT and the four cases of fixed angle systems of 36°, 32°, 38° and 34° corresponding to 1,773,234 kg/year, 1,811,370 kg/year, 1,813,112 kg/year, 1,929,187 kg/year, 1,930,543 kg/year 1,932,571 kg/year and 1,936,789 kg/year, respectively. Since the rate of electricity generation by FC is around 1 % in all systems, then almost the total GHG emissions come from the grid. Therefore, with the VSAT technique the lowest energy is purchased from the grid and the highest energy is sold to the grid as shown in Fig. 11.

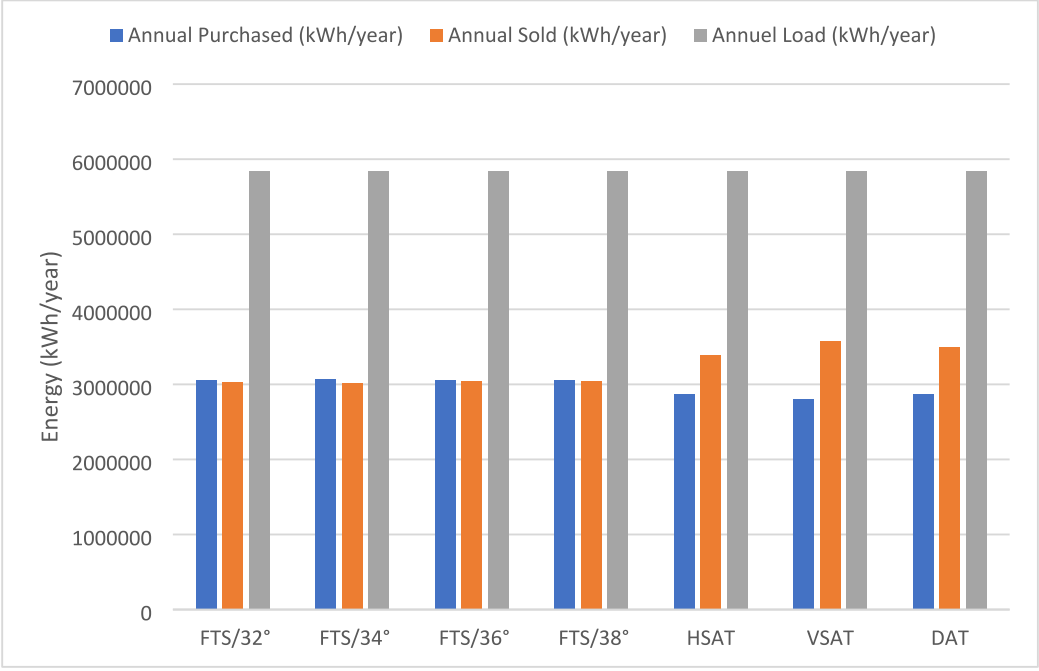

Fig. 11. Annual energy purchased/sold from/to the grid for different PV tracking techniques with annual load.

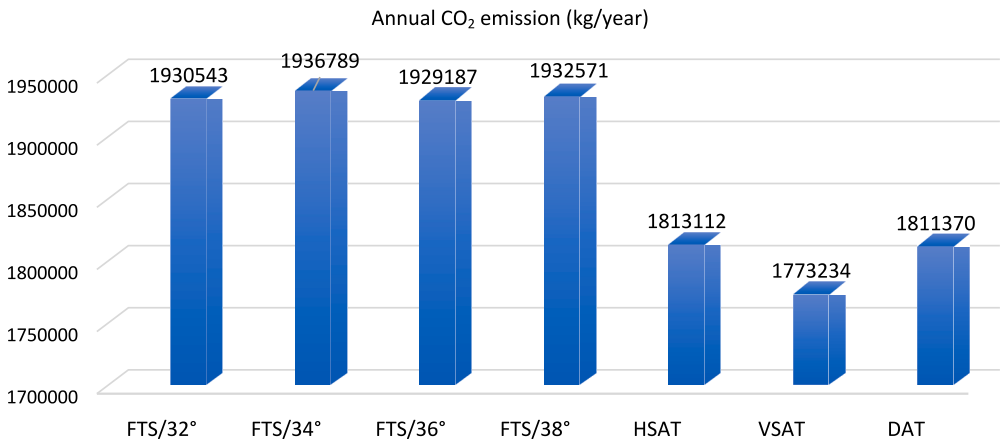

Fig. 12. CO_2 emission for different PV tracking techniques.

Based on the previous discussion regarding the technical merits of the grid-connected hybrid power system (PV-FC) with the four PV tracking techniques, it can be concluded that the VSAT is the most efficient and cost-effective solution for the location considered in this study. For the VSAT system with a PV capacity of 5,250 kW and a FC capacity of 200 kW, the annual average electricity production of PV and FC is about 75.9 % (9.23 GWh/year/year) and 0.94 % (0.11 GWh/year/year) respectively of the total generation, while the rest of the required power is purchased from the grid. In Fig. 13 shows the monthly electricity production of each component of the hybrid system.

4.2. Comparison of different PV tracking techniques on the economic aspect

HOMER calculates the NPC and COE primary economic metrics to rank various energy system configurations. The NPC calculates the present cost of the installation and the operation of the system over the project lifetime minus the present revenues, and it given by [54]:

$$NPC = \frac{C_{ann,tot}}{CRF(i,N)} \tag{6}$$

where $C_{ann,tot}$ is the total annualized cost [$/yr], N is the project lifetime [yr], i represents the annual interest rate [%] and CRF denotes the capacity recovery and is given by:

$$CRF(i,N) = \frac{i(1+i)^N}{(1+i)^N - 1} \tag{7}$$

The COE is the average cost per unit of energy (kWh) [55]. It is determined by HOMER using Eq. (8):

$$COE = (\$/kWh) = \frac{C_{ann,tot}}{R_{prim} - R_{tot,gridsales}} \tag{8}$$

where R_{prim} is the annual total cost included [kWh/an] and $R_{tot,grid,sale}$ is the total power exported to the grid [kWh/yr].

In this study, the investment period is chosen as 25 years because it is the useful lifetime commonly considered for each component of this type of installation [56]. The results of the financial analysis of the NPC and COE for each design are shown in Table 5. This table shows the total NPC and COE results of all hybrid system configurations considered in this study. The horizontal tracking scenario (HSAT) has the highest total NPC and COE due to the high investment cost since the PV capacity of this scenario is 6,000 kW (4.776 M$) which also depends on the cost of the tracking system which is $870/kW (Table 2). One option to lower the price of the system is to reduce the cost of the tracking system or decrease the PV capacity in the hybrid system.

As a result, the least cost grid-connected hybrid system VSAT is the combination of PV, FC, RF, Hydrogen Tank and Converter of capacity of 5,250 kW, 200 kW, 100 kW, 500 kg and 2,065 kW respectively. This optimum configuration is obtained by simulation using HOMER software as shown in Table 5. By applying Equations (6) and (8), HOMER calculates the NPC and COE for the entire system. The NPC of the VSAT system is 5.34 $M whereas the COE is $0.0360/kWh, with an initial investment cost (IC) of 7.11 $M. Fig. 14 shows the cost summary of VSAT hybrid system by components. The electric power purchased from the grid is considered as an operation cost, which represents the highest cost in the system. It amounts to −6.421 $M with zero unmet power demand.

Moreover, HOMER calculates other economic performance metrics such as Internal Rate of Return (IRR) and Return on Investment (ROI). The IRR is a discount rate that makes the current net cost of the base case and the current system the same. The IRR is calculated from the discount rate that makes the present value of the difference of the two cash flow sequences equal to zero. The ROI is an indication of the time it would take to recover the difference in investment costs between the current system and the reference system [33]. HOMER calculates the return on investment as follows:

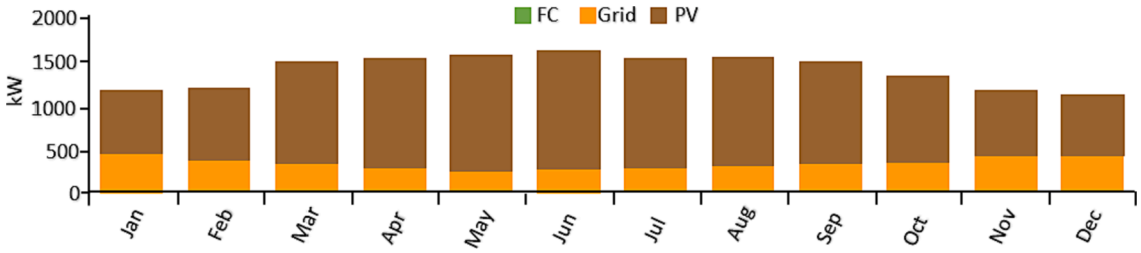

Fig. 13. Monthly generation of the PV/FC/G system.

Table 5
Different scenarios with optimization results for grid-connected hybrid system.

Parameter Scenario	PV [kW]	FC [kW]	RF [kW]	HT [kg]	Converter [kW]	NPC [$M]	COE [$/kWh]	IC [$M]
VSAT	5,250	200	100	500	2,065	5.34	0.0360	7.11
FTS/32°	5,459	200	100	500	2,065	5.68	0.0406	5.94
FTS/34°	5,417	200	100	500	2,065	5.69	0.0408	5.91
FTS/36°	5,563	200	100	500	2,065	5.70	0.0407	6.02
FTS/38°	5,568	200	100	500	2,065	5.72	0.0409	6.03
G/FC/RF	–	200	100	500	1,600	8.00	0.0870	1.41
DAT	4,834	200	100	500	2,065	8.64	0.0587	10.3
HSAT	6,000	200	100	500	2,065	10.40	0.0713	11.6

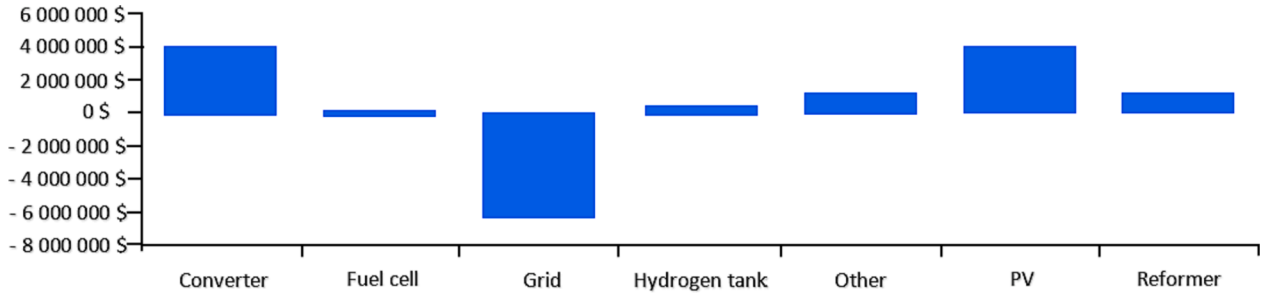

Fig. 14. Cost breakdown of various components of VSAT hybrid system.

$$ROI = \frac{\sum_{i=0}^{N} C_{i,ref} - C_i}{N\left(C_{cap} - C_{cap,ref}\right)} \tag{9}$$

where $C_{i,ref}$ is the reference system nominal annual cash flow, C_i is the current system nominal annual cash flow, C_{cap} denotes the current system capital cost and $C_{cap,ref}$ represents the reference system capital cost.

In comparison to the reference case G/FC/RF, all grid-connected PV/FC/RF systems with the distinct tracking techniques show a positive ROI and IRR as shown in Fig. 15. This is mainly due to the low cost of investment at year zero of the project G/FC/RF. The results from the financial analysis show that the most profitable system is the DAT, with an IRR = 12.9 %, followed by the VSAT with IRR = 12.1 %. The worst investment is the FTS/38°, with a very low value of IRR = 9.2 %. On the other hand, the lowest ROI is 6.3 % achieved with the FTS/38° system which can generate extra power and sell it to the grid. The highest ROI of 9.5 % was obtained with the DAT system with the shortest simple payback (SP) repayment period of 7.38 years which makes it the best option since it makes a profit during the project's lifetime. It is followed by the VSAT with a value of ROI = 8.8 % and a SP repayment period of 7.79 years. It should be emphasized that PV solar tracker prices are expected to continue to decline over the next few years, it is expected that the ongoing reduction in production costs and market expansion will continue in the future. As a result, all trackers system will have a higher ROI.

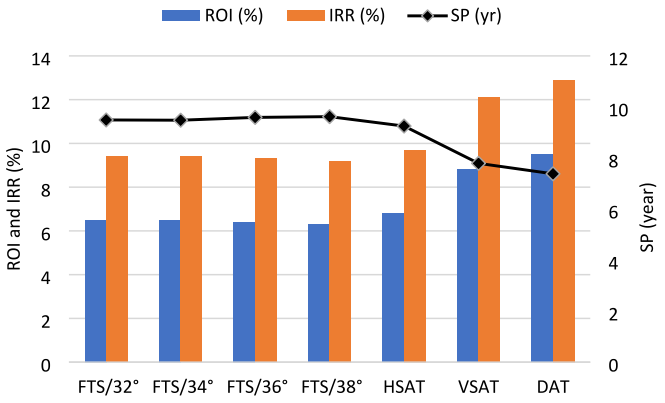

Fig. 15. ROI - IRR and Simple Payback (SP) with G/FC/RF as the reference case.

4.3. Optimal grid-connected PV/RF/FC hybrid system operation status with best PV tracking technique

The software HOMER finds the best mix of resources at the lowest cost over the project lifetime, which ensures that the load requirements are met by the hybrid power system. In this section, the performance of the optimal grid-connected PV/RF/FC hybrid system with VSAT is discussed. This system has the lowest NPC of 5.34 $M. The optimal system components size are: PV power of 5,250 kW, reformer power of 100 kW, hydrogen tank capacity of 500 kg, FC power of 200 kW, inverter power rating of 2,065 kW, power purchased and power sold to the grid annually are 2.81 GW and 3.57 GW respectively.

4.3.1. Cash flow by component and cost type

The cash flow of the optimal HES listed by component and cost type, obtained from HOMER software are shown in Fig. 16(a) and (b) respectively. The following conclusions can be drawn from these results:

- The initial capital cost of a component is the total installed cost at time zero of the lifetime of the system for all the components. It is the total installation cost of that component at the beginning of the project, which includes: the PV generators, the FC, the reformer, the other (PV solar tracker), the grid connection, the hydrogen tank and the power converters as shown in Fig. 16(a).
- The replacement cost is the cost of replacing a component and includes the disposal cost of the waste at the end of its lifetime, as specified by the lifetime parameter in the component model. This cost can be different from the initial capital cost. Fig. 16(b) clearly shows that the replacement cost is at the 20th year of the project lifetime only for the power converters with the value of −413,000 $.
- The Operation and Maintenance (O&M) cost of a component is the cost associated with operating and maintaining that component. The total O&M cost of the system is the sum of the O&M costs of each system component. It is shown in Fig. 16(b) that the O&M annual

a)

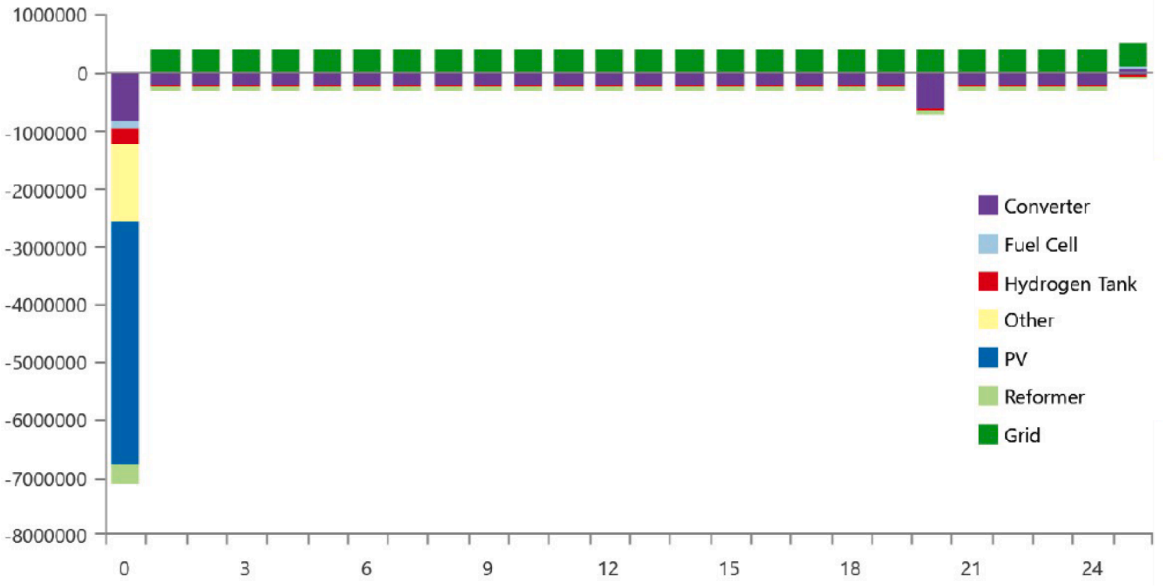

b)

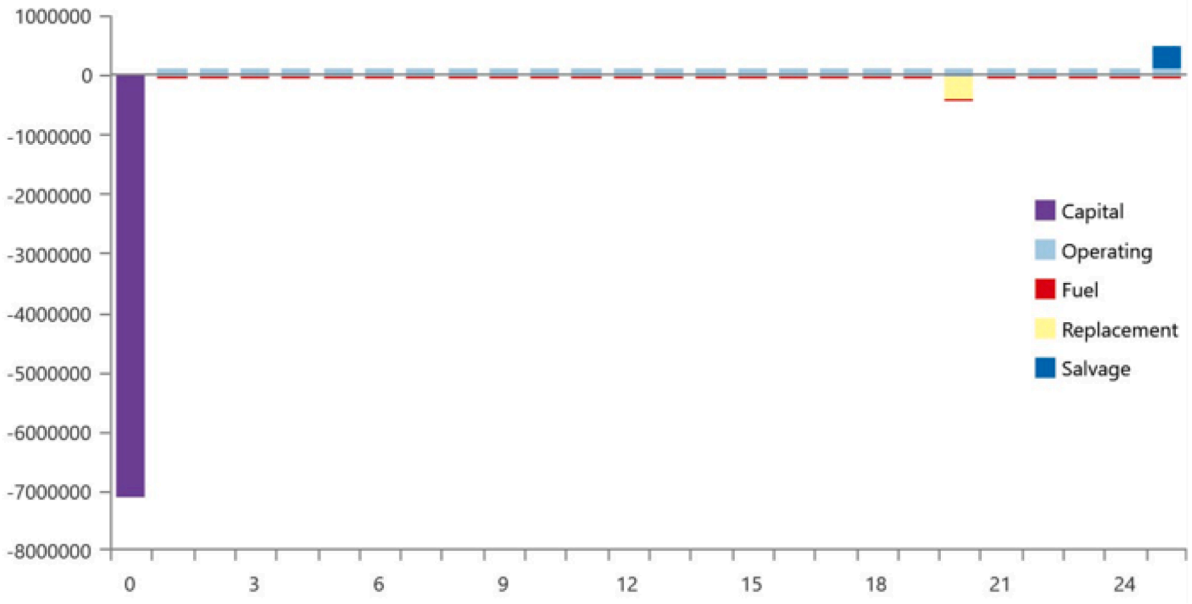

Fig. 16. Cash flow of the optimum system listed by (a) component, (b) cost type.

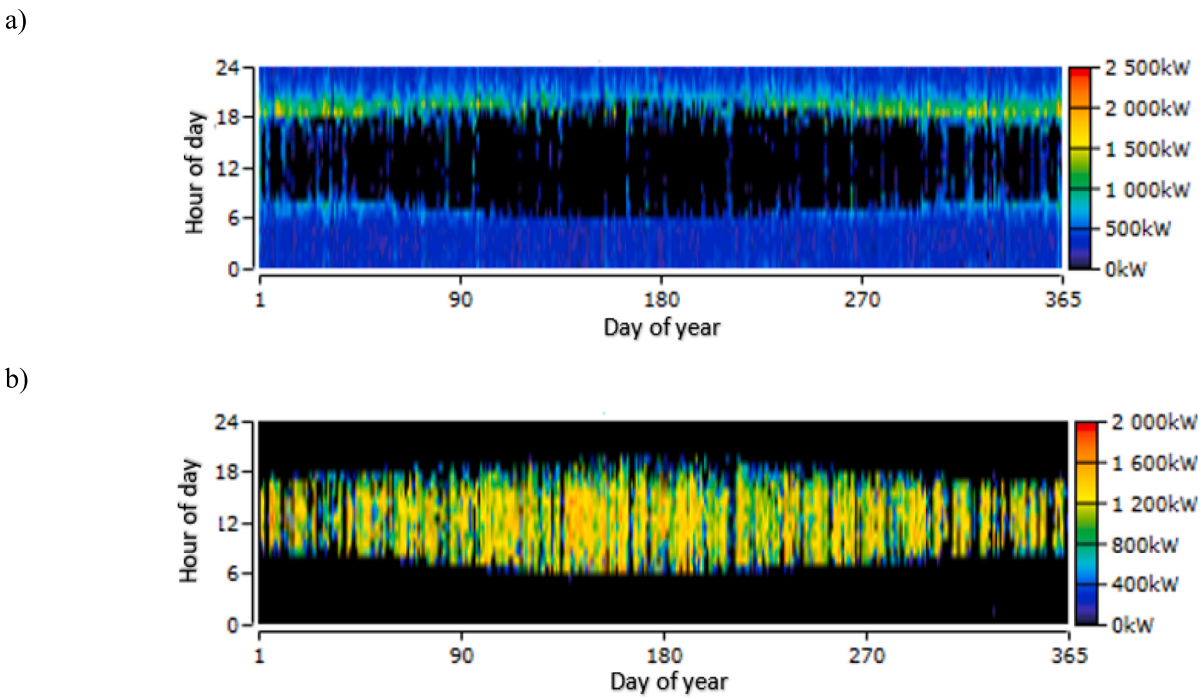

Fig. 17. A) daily data through the year of energy purchased, b) energy sold to the grid usingvsat.

costs over the life of the project have positive value of 156,681 $, given that the grid O&M cost (407,622 $) which is equal to the annual cost of buying electricity from the grid minus any income from the export of electricity to the grid is greater than the sum of the rest of the other O&M cost of components such as converter (-206,500 $), fuel cell (-9,440 $), hydrogen tank (−15,000 $) and reformer (−20,000 $).

- Fuel cost is calculated by multiplying the fuel price by the amount of fuel used by the generator in one year. It is obvious that the reformer is the only component that consumes fuel (natural gas) with an annual value of 41,170 $ during the project lifetime as shown in Fig. 16(b).

- Salvage value is the value that remains in the components of the energy system at the end of the project's lifetime. HOMER assumes linear depreciation of components, meaning that the salvage value of a component is directly proportional to its remaining life. It is clearly depicted in Fig. 16(a), (b) that, after 25 years, the optimal grid-connected hybrid system is expected to end with a total of 372,875 $ as salvage costs, 63,125 $ for FCs and 309,750 $ for power converter.

4.3.2. Technical analysis by component

4.3.2.1. Grid electrical summary. The grid is the main source of electricity generation. It supplies the system day and night, in summer and winter. Furthermore, the VSAT hybrid system resells energy to the grid during the day with a maximum rate in summer than in winter. A type of graph forms a data map (DMap) showing one year of time series data of energy flow from/to the grid is shown in Fig. 17(a), (b) for the energy purchased and sold, respectively.

4.3.2.2. PV electrical summary. A 5,250 kW of PV was found to be the optimal size of the hybrid VSAT system for the neighborhood of the City of Chlef (Algeria) considered in this study. Table 6 presents a summary of the PV output results during the project lifetime, which provides essential information regarding the quantity of PV output for Chlef region. Fig. 18 shows the PV power generation when operated 4389 hrs/yr during daylight which is longer in the summer than winter and the peak power output appeared around 13:00 pm.

Table 6
Summary of PV output results.

Rated capacity (kW)	5,250
Mean output (kW)	1,054
Mean output (kWh/d)	25,295
Capacity factor (%)	20.1
Minimum output (kW)	0
Maximum output (kW)	4,716
Hours of operation (hrs/yr)	4,389
Total production (kWh/yr)	9,232,824

4.4.3.2.3. Fuel cell electrical summary. A FC of 200 kW was found to be the most appropriate for the hybrid VSAT system to satisfy the load requirements. Table 7 summarizes the simulation results of the FC output. The FC behaves like a backup power generation, it operates 590 hrs/yr and produces 114,295 kWh/yr which corresponds to only a small fraction of power production. From Fig. 19, it can be observed that the FC rarely operates during the day throughout the year, but it operates early in the day to meet unexpected power demand.

4.4.3.2.4. Reformer summary. A reformer of 100 kg/hr capacity was found to be the optimal size to supply the tank with hydrogen in the HES based on VSAT. Table 8 summarizes the simulation results of the RF output. The RF operated 2,841 h per year. It starts at sunrise and operates till around midnight, as shown in Fig. 20. The total hydrogen production over a year is 267,490 kg/yr where the average output production is 30.5 kg/hr. The cost of hydrogen is 1.27 $/kg as defined by HOMER. The hydrogen storage level depends on the RF and FC operation. The hydrogen level decreases when the FC is operating and increases when the FC is idle and the reformer is operating.

4.4.3.2.5. Hydrogen tank summary. A tank with a capacity storage range 0–500 kg was considered as the optimal size to store hydrogen for the supply of the FC. A summary of results according to hydrogen-tank production and consumption is presented in Table 9. It reveals that there is a 417 kg surplus of hydrogen every year. The level of the tank decreases when the FC is operating, and this allows the RF to produce hydrogen to fill-in the tank again. Fig. 21 illustrates that the variation of the amount of hydrogen stored corresponds to the operation of the FC

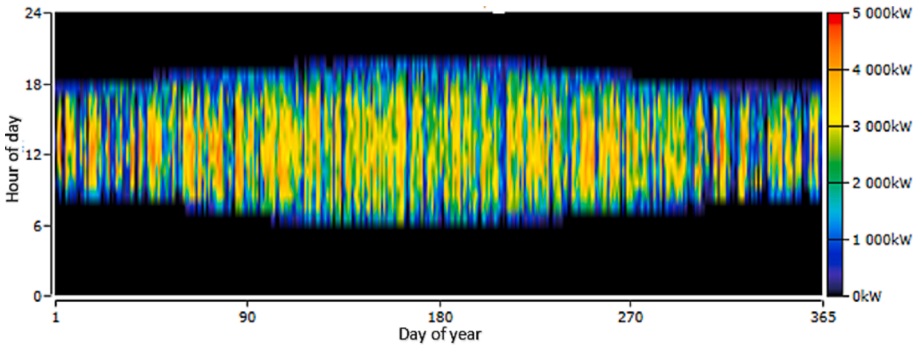

Fig. 18. PV power output throughout the year for the VSAT system.

Table 7
Summary of FC output results.

Hours of operation (hrs/yr)	590
Operational life (yr)	67.8
Capacity factor (%)	6.52
Electrical production (kWh/yr)	114,295
Mean electrical output (kW)	194

and the reformer.

4.4.3.2.6. Converter electrical summary. A 2,065-kW inverter was determined to be the optimal size of VSAT hybrid system. Table 10 summarizes the results of the inverter performance in the simulation. The time of operation of the converter as an inverter during the year is 4,381 h. Fig. 22 shows the hours/days of the inverter output power.

8. Conclusions

In this research, an attempt has been made to study the feasibility of a grid-connected PV/Reformer/FC hybrid system with four distinct sun tracking designs including HSAT, VSAT, DAT and FTS with four different angles (32°, 34°, 36°, 38°) to meet the electrical load demand of an agglomeration in the City of Chlef in Algeria. The modeling and optimization of the hybrid power system were carried out using HOMER Pro software. The input data such as weather conditions (solar irradiation and ambient temperature) were collected in the studied location during the year 2020 and the load demand of the agglomeration was estimated at 16,000 kWh/day with a peak of 2.163 MW. In addition, the technical and economic data of the components of the hybrid system have been provided by the manufacturers. The simulation results were used to assess and analyze the technical and economic performance of the different system configurations. Based on the analysis presented in this paper, the following are the key findings:

- *Annual energy production*: The results show that the VSAT has the highest power production followed by HSAT, DAT and FTS respectively.
- *Annual FC power generation*: It is found that the fuel cell rarely operates during the year and it is only used to compensate the energy lack during the night and peak season.
- *Total annual PV generation*: The results showed that the VSAT system produced 1.49 %, 3.14 %, 18.01 %, 18.16 %, 20.05 % and 21.02 more power than the HSAT, DAT and FTS (36°, 38°, 32°, 34°) respectively.
- *Energy excess to be fed back into the grid*: The HSAT produced the highest amount, 39 %, 12.60 % and 5.59 % more than FTS, DAT and

Table 8
Summary of RF output results.

Rated capacity (kg/hr)	100
Hydrogen production (kg/yr)	267,490
Mean hydrogen output (kg/hr)	30.5
Capacity Factor (%)	0.305
Minimum output (kg/hr)	0
Maximum output (kg/hr)	100
Hours of operation (hrs/yr)	2,841

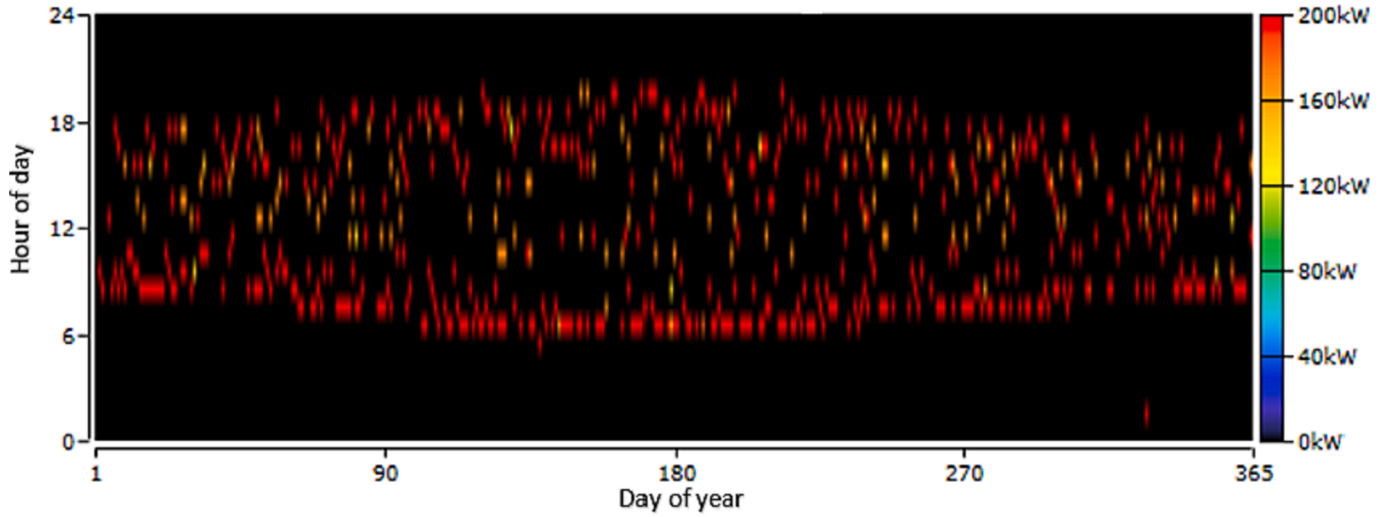

Fig. 19. FC power output throughout the year for the VSAT system.

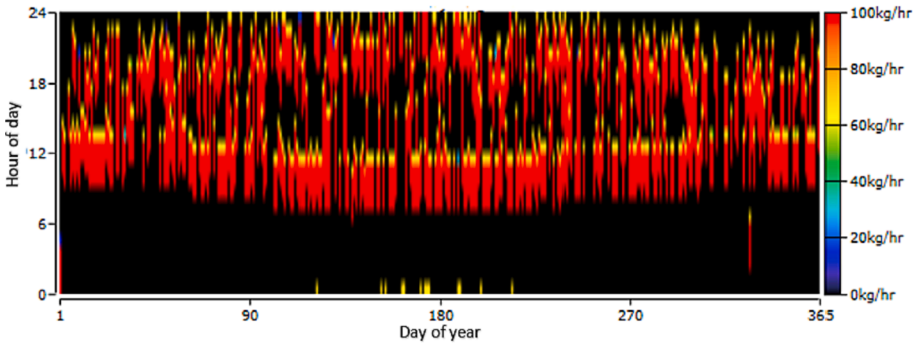

Fig. 20. Reformer hydrogen output throughout the year for the VSAT system.

Table 9
Summary of the hydrogen tank results.

Hydrogen production (kg/yr)	267,490
Hydrogen consumption (kg/yr)	267,073
Hydrogen tank autonomy (hrs)	25

VSAT respectively. All fixed angle systems (32°, 34°, 36°and 38°) produced similar amounts of excess of electricity.

- *PV penetration*: The result revealed that the VSAT system recorded higher penetration of solar power to the grid of 158 %, followed by HSAT, DAT and FTS, which recorded 156 %, 153 %, and 131 %, respectively.
- *Annual energy sold to the grid:* The VSAT system showed the highest value followed by DAT, HSAT and FTS respectively.
- *Annual CO_2 emission*: The VSAT showed the lowest value, while FTS presented the highest annual CO_2 emission value followed by HSAT, DAT. In addition, almost all GHG emissions come from energy purchased from the grid. Within this framework, the VSAT has the lowest environmental impacts.
- *Financial analysis*: The results of this study showed that VSAT system has the lowest NPC and COE, 5.34 $M and 0.0360 $/kWh respectively. This is mainly due to the relatively low power generation cost along despite the high initial investment cost an estimated value of 7.11 $M.
- *Economic performance metrics performed against the reference case G/FC/RF*: The results have shown that the most profitable system is the DAT with a value of IRR = 12.9 %, followed by the VSAT with a value of IRR = 12.1 % and the low ROI is found in the FTS/38° system which is 6.3 % with a value of IRR = 9.2 %. Eventually, DAT recorded the highest ROI of 9.5 % and a shortest simple payback (SP) repayment period of 7.38 years which makes it the best option since it makes a profit during the project's lifetime (25 years), followed by the VSAT with a value of ROI = 8.8 % and a SP repayment period of 7.79 years.

From the results of the study, it can be concluded that the HES (Hybrid Energy System) based on the VSAT is the most economically, technically, and environmentally feasible solar tracking system for the agglomeration considered. This system has the lowest NPC and the COE, highest total electricity generation where the surplus of generation can be exported to the grid, as well as the lowest CO_2 emissions due to high penetration of renewable energy. To conclude, this paper presents a comprehensive analysis of the feasibility, technical and economics performances of grid-connected PV/Reformer/FC hybrid system with different Photovoltaic (PV) tracking systems. The possible directions for future work would be (i) performance analysis of a large-scale hybrid grid-connected system for various sites under different meteorological conditions (ii) Introduction of real price for the sale and purchase of electricity to/from the grid (iii) Implementation of the designed hybrid energy model in a real-life case study.

CRediT authorship contribution statement

Mohamed Dekkiche: Methodology, Software, Writing – original draft, Investigation, Formal analysis, Validation. **Toufik Tahri:** Supervision, Investigation, Formal analysis, Writing – review & editing. **Mouloud Denai:** Formal analysis, Writing – review & editing.

Declaration of Competing Interest

The authors declare that they have no known competing financial interests or personal relationships that could have appeared to influence the work reported in this paper.

Data availability

The data that has been used is confidential.

Table 10
Summary of the inverter results.

Capacity (kW)	2,065
Mean output (kW)	760
Capacity factor (%)	36.8
Hours of operation (hrs/yr)	4,381
Energy out (kWh/yr)	6,655,561
Energy in (kWh/yr)	7,005,538
Losses (kWh/y)	350,277

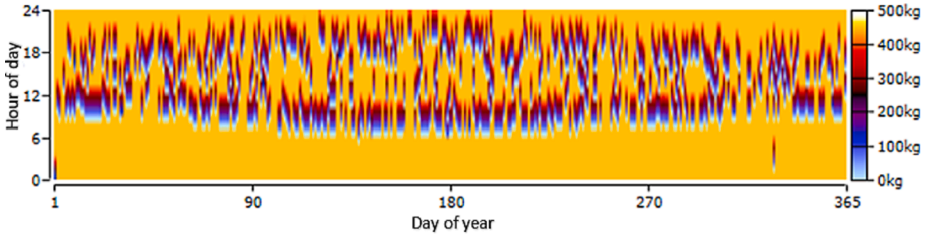

Fig. 21. Tank hydrogen level throughout the year for the VSAT system.

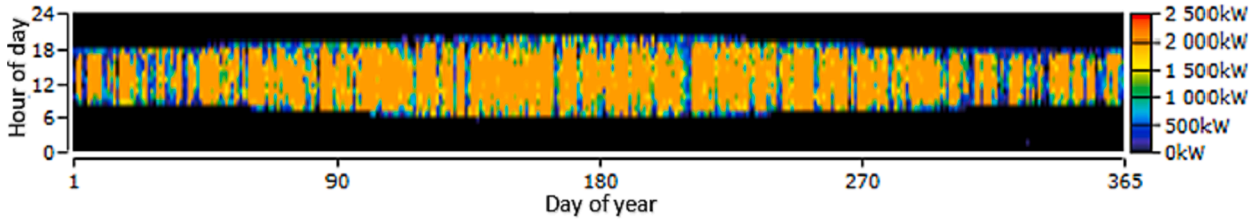

Fig. 22. Inverter power output throughout the year for the VSAT system.

References

[1] S Eddrief-Cherfi, Renewable energy in Algeria, What alternatives to fossil fuels, Solar, nuclear or both at the same time, La Revue de l'Énergie. 609 (2012) 372–387. https://inis.iaea.org/search/search.aspx?orig_q=RN:44026705#.

[2] Weiqiang D, Yanjun L, Ji X. Optimal sizing of a stand-alone hybrid power system based on battery/hydrogen with an improved ant colony optimization. Energies 2016;9:785. https://doi.org/10.3390/en9100785.

[3] Torreglosa JP, García P, Fernández LM, Jurado F. Energy dispatching based on predictive controller of an off-grid wind turbine/photovoltaic/hydrogen/battery hybrid system. Renew Energy 2015;74:326–36. https://doi.org/10.1016/j.renene.2014.08.010.

[4] Cervantes I, Hernandez-Nochebuena M, Cano-Castillo U, Araujo-Vargas I. A graphical approach to optimal power management for uncertain OFF-Grid PV-FC-electrolyzer-battery hybrid systems. Int J Hydrog Energy 2018. https://doi.org/10.1016/j.ijhydene.2018.08.167.

[5] Hwang JJ, Lai LK, Wu W, Chang WR. Dynamic modeling of a photovoltaic hydrogen fuel cell hybrid system. Int J Hydrog Energy 2009;34:9531–42. https://doi.org/10.1016/j.ijhydene.2009.09.100.

[6] Marchenko OV, Solomin SV. Modeling of hydrogen and electrical energy storages in wind/PV energy system on the Lake Baikal coast. Int J Hydrog Energy 2017;42:9361–70. https://doi.org/10.1016/j.ijhydene.2017.02.076.

[7] M. O. Hazem, Y. Amirat, M. Benbouzid, A. A. Elbaset, Optimal design of a PV/fuel cell hybrid power system for the city of Brest in France, in: 2014 First Int. Conf. Green Energy ICGE 2014. (2014) 119–123. 10.1109/icge.2014.6835408.

[8] M. S. Alam, D. W. Gao, Modeling and Analysis of a Wind/PV/Fuel Cell Hybrid Power System in HOMER, in: 2nd IEEE Conf. Ind. Electron. Appl. (2007) 1594–1599. 10.1109/iciea.2007.4318677.

[9] Das HS, Tan CW, Yatim AHM, Lau KY. Feasibility analysis of hybrid photovoltaic/battery/fuel cell energy system for an indigenous residence in East Malaysia. Renew Sust Energy Rev 2017;76:1332–47. https://doi.org/10.1016/j.rser.2017.01.174.

[10] Ramli MAM, Hiendro A, Sedraoui K, Twaha S. Optimal sizing of grid-connected photovoltaic energy system in Saudi Arabia. Renew Energy 2015;75:489–95. https://doi.org/10.1016/j.renene.2014.10.028.

[11] Das D, Esmaili R, Xu L, Nichols D. An optimal design of a grid connected hybrid wind/photovoltaic/fuel cell system for distributed energy production. Annu Conf IEEE Ind Electron Soc 2005. https://doi.org/10.1109/iecon.2005.1569298.

[12] S. Z. Hassan, S. Mumtaz, T. Kamal, L. Khan, Performance of grid-integrated photovoltaic/fuel cell/ electrolyzer/battery hybrid power system, in: Power Gener. Syst. Renew. Energy Technol. (2015) 1–8. 10.1109/PGSRET.2015.7312249.

[13] Batman A, Bagriyanik FG, Aygen ZE, Gül Ö, Bagriyanik M. A feasibility study of grid-connected photovoltaic systems in Istanbul. Turkey Renew Sust Energy Rev 2012;16:5678–86. https://doi.org/10.1016/j.rser.2012.05.031.

[14] Wu W, Christiana VI, Chen S-A, Hwang J-J. Design and techno-economic optimization of a stand-alone PV (photovoltaic)/FC (fuel cell)/battery hybrid power system connected to a wastewater-to-hydrogen processor. Energy 2015;84:462–72. https://doi.org/10.1016/j.energy.2015.03.012.

[15] Dadak A, Mousavi SA, Mehrpooya M, Kasaeian A. Techno-economic investigation and dual-objective optimization of a stand-alone combined configuration for the generation and storage of electricity and hydrogen applying hybrid renewable system. Renew Energy 2022;201:1–20. https://doi.org/10.1016/j.renene.2022.10.085.

[16] Talavera DL, Muñoz-Cerón E, Ferrer-Rodríguez JP, Pérez-Higueras PJ. Assessment of cost-competitiveness and profitability of fixed and tracking photovoltaic systems: the case of five specific sites. Int Renew Energy 2019;134:902–13. https://doi.org/10.1016/j.renene.2018.11.091.

[17] Hoffmann FM, Molz RF, Kothe JV, Benitez Nara EO, Carvalho Tedesco LP. Monthly profile analysis based on a two-axis solar tracker proposal for photovoltaic panels. Renew Energy 2018;115:750–9. https://doi.org/10.1016/j.renene.2017.08.079.

[18] Mirzaei M, Mohiabadi MZ. Comparative analysis of energy yield of different tracking modes of PV systems in semiarid climate conditions: the case of Iran. Renew Energy 2018;119:400–9. https://doi.org/10.1016/j.renene.2017.11.091.

[19] Yaichi M, Tayebi A, Mammeri A, Boutadara A. Performance of a PV field's discontinuous two-position sun tracker systems supplying a water pumping system: concept, theoretical and experimental studies – A case study of the Adrar area in Algeria's Sahara. Renew Energy 2022;201:548–62. https://doi.org/10.1016/j.renene.2022.10.095.

[20] Ngo XC, Nguyen TH, Do NY, Nguyen DM, Vo DN, Lam SS, et al. Grid-connected photovoltaic systems with single-axis sun tracker: case study for central vietnam. Energies 2020;13(6):1457. https://doi.org/10.3390/en13061457.

[21] Alktranee MHR, Al-Yasiri Q, Sahib MM. Power output enhancement of grid-connected PV system using dual-axis tracking. J Renew Energy Environ Sustain 2020;5:8. https://doi.org/10.1051/rees/2020002.

[22] Liu Y, Gong M, Liang L, Liu Q, Gao Y. Research and design of low-power grid-connected PV power generation system based on automatic solar tracking. Syst Sci Control Eng 2018;6:278–88. https://doi.org/10.1080/21642583.2018.1553692.

[23] Babatunde OM, Munda JL, Hamam Y. Off-grid hybrid photovoltaic – micro wind turbine renewable energy system with hydrogen and battery storage: effects of sun tracking technologies. Energy Convers Manage 2022;255:115335. https://doi.org/10.1016/j.enconman.2022.115335.

[24] Mubaarak S, Zhang D, Chen Y, Jinxin L, Wang L, Rongfang Y, et al. Techno-economic analysis of grid-connected PV and fuel cell hybrid system using different PV tracking techniques. Appl Sci 2020;10:8515. https://doi.org/10.3390/app10238515.

[25] Bendaoud B, Malek A, Loukarfi L, Mammeur H. Conceptual study of photovoltaic power plant connected to the urban electrical network in northern Algeria, in. Energy Sources A: Recovery Util Environ Eff 2020:1–20. https://doi.org/10.1080/15567036.2020.1758852.

[26] Alharthi Y, Siddiki M, Chaudhry G. Resource assessment and techno-economic analysis of a grid-connected solar PV-wind hybrid system for different locations in Saudi Arabia. Sustainability 2018;10:01–22. https://doi.org/10.3390/su10103690.

[27] https://www.condor.dz/images/pdf/CatalogueProduitsSolairesPhotovoltaiques_min.pdf. (accessed 21 December 2021).

[28] Les Dossiers de La Lettre du Solaire. Mai 2014 / Vol 5 N°05, Programmes PED, Publiée par CYTHELIA sas. (accessed 21 December.2021).

[29] Al Garni HZ, Awasthi A, Ramli MAM. Optimal design and analysis of grid-connected photovoltaic under different tracking systems using HOMER. Energy Convers Manage 2018;155:42–57. https://doi.org/10.1016/j.enconman.2017.10.090.

[30] P. E. Dodds, Economics of d'hydrogen production, in: Compendium de l'énergie de l'hydrogène, (2015) 63–79.

[31] Bendaikha W, Touafek K, Serir L. Etude d'une Installation à Base d'une Pile à Combustible pour l'Alimentation en Energie d'une Habitation. Rev Energ Ren ICPWE 2003:79–81.

[32] https://www.ifpenergiesnouvelles.fr/enjeux-et-prospective/decryptages/energies-renouvelables/tout-savoir-lhydrogene, (accessed 21 December 2021).

[33] Manuel utilization Homer Energy (2016) HOMER Pro Version 3.7, Colorado.

[34] Vaziri Rad MA, Ghasempour R, Rahdan P, Moosavi S, Arastounia M. Techno-economic analysis of a hybrid power system based on the cost-effective hydrogen production method for rural electrification, A case study in Iran, in. Energy 2019. https://doi.org/10.1016/j.energy.2019.116421.

[35] Isa NM, Das HS, Tan CW, Yatim AHM, Lau KY. A techno-economic assessment of a combined heat and power photovoltaic/fuel cell/battery energy system in Malaysia hospital. Energy 2016;112:75–90. https://doi.org/10.1016/j.energy.2016.06.056.

[36] https://fr.globalpetrolprices.com/Algeria/natural_gas_prices/, (accessed 21 December 2021).

[37] Alazemi J. Automotive Solar Hydrogen Fuelling Stations: Concept Design, Performance Testing and Evaluation. RMIT University; 2016.

[38] G Zini, P. Tartarini, Solar Hydrogen Energy Systems, in: Science and Technology for the Hydrogen Economy, Springer, 2011.

[39] Gökçek M, Kale C. Techno-economical evaluation of a hydrogen refuelling station powered by Wind-PV hybrid power system: a case study for İzmir-Çeşme. Int J Hydrog Energy 2018;43:10615–25. https://doi.org/10.1016/j.ijhydene.2018.01.082.

[40] R. O'hayre, S-W. Cha, W. Colella, F. B. Prinz, J. Wiley, Sons, Fuel cell fundamentals. 2nd edition, 2006.

[41] E. F. Curd and C. A. Howard, Introduction to Building Services, in: Macmillan International Higher Education, 2nd edition, 1996.

[42] Fred H, Greeno R. Building services handbook. Routledge 2017. https://doi.org/10.4324/9781315276977.

[43] S. R. Perumal, F. Baharum, M. N. M. Nawi, M. F. Omar, Photovoltaic Potential Analysis - Fuel Cell Hybrid Energy System for General-Purpose Building of Laboratory and Offices Using HOMER Software, J. Adv. Res. Fluid Mech. Therm. Sci. 2 (2021) 63–81. 10.37934/arfmts.84.2.6381.

[44] https://www.homerenergy.com/pdf/HOMERHelpManual.pdf.

[45] https://www.homerenergy.com/products/pro/docs/latest/index.html.

[46] https://www.google.com/maps Chlef Algeria, (accessed 21 December 2021).

[47] G. Bekele, The study into the potential and feasibility of standalone solar-wind hybrid electric energy supply system for application in Ethiopia, in: KTH Royal Institute of Technology, Stockholm. Sweden. 2009.

[48] Dekkiche M, Tahri T, Bettahar A, Belmadani B. Weather data analysis and optimal design of hybrid PV-wind-diesel power system for a village in Chlef, desalination. Water Treat 2017;79:125–34. https://doi.org/10.5004/dwt.2017.20714.
[49] Gairaa K, d S. Benkaciali,. Analysis of solar radiation measurements at Ghardaïa area, south Algeria. Energy Procedia 2011;6:122–9. https://doi.org/10.1016/j.egypro.2011.05.014.
[50] https://www.controle-gaz.be/les-10-principaux-pays-producteurs-de-gaz-naturel/.
[51] https://www.algerie-eco.com/2022/01/16/production-petrole-2021/.
[52] https://unfccc.int/resource/docs/natc/algnc1.pdf.
[53] Hamiti D, Bouzadi-Daoud S. The algerian energy transition strategy in line with the renewable energy development and energy efficiency program: situation and prospective of development. J Contemp Account Econ 2021;04.
[54] Hiendro A, Kurnianto R, Rajagukguk M, Simanjuntak YM. Junaidi, Techno-economic analysis of photovoltaic/wind hybrid system for onshore/remote area in Indonesia. Energy 2013;59:652–7. https://doi.org/10.1016/j.energy.2013.06.005.
[55] Rezk H, Sayed ET, Al-Dhaifallah M, Obaid M, El-Sayed AHM, Abdelkareem MA, et al. Fuel cell as an effective energy storage in reverse osmosis desalination plant powered by photovoltaic system. Energy 2019;175:423–33. http://doi:10.1016/j.energy.2019.02.167.
[56] Miguel SM, Cristina AT, Montserrat DM. Performance indicators for sun-tracking systems: a case study in spain. Energy Power Eng 2014;6:292–302. https://doi.org/10.4236/epe.2014.69025.